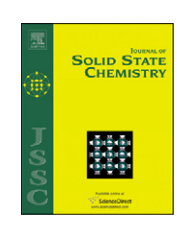
FI SEVIER

Contents lists available at SciVerse ScienceDirect

### Journal of Solid State Chemistry

journal homepage: www.elsevier.com/locate/jssc



# Preparation and photocatalytic activity for water splitting of Pt-Na<sub>2</sub>Ta<sub>2</sub>O<sub>6</sub> nanotube arrays

Jing Liu<sup>a</sup>, Jiawen Liu<sup>a,\*</sup>, Zhonghua Li<sup>b,\*\*</sup>

- <sup>a</sup> Key Laboratory for Photonic and Electronic Bandgap Materials, Ministry of Education, and College of Chemistry and Chemical Engineering, Harbin Normal University, Harbin 150025, PR China
- b Key Laboratory of Microsystems and Microstructures Manufacturing, Ministry of Education, Harbin Institute of Technology, Harbin 150001, PR China

#### ARTICLE INFO

Article history:
Received 29 June 2012
Received in revised form
3 October 2012
Accepted 9 October 2012
Available online 18 October 2012

Keywords: Na<sub>2</sub>Ta<sub>2</sub>O<sub>6</sub> nanotube arrays Ta<sub>2</sub>O<sub>5</sub> nanotube arrays Photocatalysis Water splitting

#### ABSTRACT

 $Na_2Ta_2O_6$  nanotube arrays were prepared by hydrothermal method from  $Ta_2O_5$  nanotube arrays, obtained by anodization of Ta foils, in  $Na_2CO_3$  solution at 150 °C. The as-synthesized samples were characterized by X-ray diffraction (XRD), scanning electron microscope (SEM), UV-vis diffuse reflectance spectra (UV-DRS) and X-ray photoelectron spectroscopy (XPS). Analysis results show that pyrochlore structure  $Na_2Ta_2O_6$  nanotube arrays have been successfully fabricated. The diameters and lengths of  $Na_2Ta_2O_6$  nanotube arrays are 50 nm and 4  $\mu$ m, respectively. The photocatalytic hydrogen production activities of the as-synthesized  $Na_2Ta_2O_6$  nanotube arrays are highly dependent on the hydrothermal reaction time and  $Na_2CO_3$  concentration, optimized reaction parameters are obtained. To further improve the photocatalytic activity for hydrogen evolution, Pt loaded  $Na_2Ta_2O_6$  nanotube arrays are prepared by photochemical reduction method. The Pt loaded samples exhibit much higher activity for hydrogen evolution than pure  $Na_2Ta_2O_6$  nanotube arrays. Moreover, the photocatalytic hydrogen properties are rather stable.

© 2012 Elsevier Inc. All rights reserved.

#### 1. Introduction

Extensive fossil fuel consumption and environmental pollution are the two major problems for the human society. It is therefore necessary to develop a new clean and renewable energy resource in order to solve the issues. Hydrogen is considered as an ideal fuel to replace fossil fuels in the future [1–3]. Among the various approaches for hydrogen production, photocatalytic water splitting using semiconductors and solar energy has been regarded as the most promising approach [4–6].

For the past few years, there has been increasing interest in development of photocatalysis, but the number of photocatalyst materials is yet limited. Among the reported semiconductor photocatalysts, TiO<sub>2</sub> and MTiO<sub>3</sub> have been extensively studied [7–10]. Recently, tantalates have been reported as active photocatalysts for water splitting [11–18]. Most of tantalates showed high photocatalytic activities for water splitting. Particularly, NiO/NaTaO<sub>3</sub> doped with La showed the highest activity due to the appropriate conduction band level and delocalization caused by the proper distortion of TaO<sub>6</sub> connection. Therefore, it is worthwhile to investigate tantalate photocatalysts for water splitting. However, most investigations have focused on the powder-form photocatalysts and it is difficult to

separate out them from the solutions. Consequently, the development of semiconductor photocatalyst thin films has drawn much attention due to their recycle. Recently, tantalate thin films with pyrochlore structure have been reported for efficient hydrogen production under ultraviolet (UV) [19]. Furthermore, the nanotube-array architecture also affects the photocatalytic activity because of their high specific areas and efficient charge transfer [20]. Such a tubular structure increases the light scattering which results in the increase of the light absorption and the enhancement of conversion efficiency [21]. Therefore, it is highly desirable to prepare tantalate nanotube array films.

In this paper,  $Na_2Ta_2O_6$  nanotube arrays were successfully prepared by hydrothermal method using  $Ta_2O_5$  nanotube arrays as precursor, obtained by anodization of Ta foils. It is known that loading of noble metals on the surface of photocatalysts may rapidly transfer photogenerated electron from semiconductor to the noble metal particles, resulting in the enhancement of photocatalytic activities [22–28]. Therefore,  $Pt-Na_2Ta_2O_6$  nanotube array thin films were also fabricated by photochemical reduction method. Moreover, their photocatalytic performances for hydrogen production from methanol aqueous solution were also studied.

#### 2. Experimental

#### 2.1. Photocatalyst preparation

Tantalum foils (99.9% purity,  $2 \times 4$  cm) were polished by abrasive papers, and then ultrasonically cleaned in acetone and

 $<sup>^{*}</sup>$  Corresponding author. Fax:  $+86\,451\,88060653$ .

<sup>\*\*</sup> Corresponding author.

E-mail addresses: jiawenliu@yahoo.com.cn, jwliu@hrbnu.edu.cn (J. Liu), lizh@hit.edu.cn (Z. Li).

deionized water. This procedure was followed by rinsing with deionized water and drying in air. The electrochemical setup consisted of a two-electrode configuration with platinum as a counter electrode and a direct current power source. The samples were anodized in  $3\%HF+8\%H_2O+H_2SO_4$  at 25 V for 20 min. All anodization experiments were carried out at room temperature. After anodization, the anodized samples were rinsed in deionized water and dried in flowing air.

Then  $Ta_2O_5$  nanotube arrays obtained by anodization of Ta foils were used as templates to form  $Na_2Ta_2O_6$  nanotube arrays by hydrothermal method. The hydrothermal synthesis was performed as follows: the anodized Ta foils were immersed in different concentration of sodium carbonate solutions prepared in  $CO_2$ -free deionized water. Then, the hydrothermal vessels were heat-treated at 150 °C for 2 to 24 h. Finally, the samples were removed from the hydrothermal vessels, rinsed in deionized water and dried.

In order to load Pt on the surface of  $Na_2Ta_2O_6$  nanotube array film,  $Na_2Ta_2O_6$  nanotube array film was put into a vacuum oven at 60 °C after 4 mM  $H_2PtCl_6$  was spread on it. Then the sample was irradiated by a 350 W high-pressure Hg lamp in 50 mL methanol for 30 min to reduce  $Pt^{2+}$  ions. Finally, Pt loaded  $Na_2Ta_2O_6$  nanotube array film was obtained. For the typical sample used for the measurement of XPS and DRS, the content of Pt is 2  $\mu$ mol.

#### 2.2. Photocatalyst characterization

The structures and morphologies of the prepared samples were characterized by field emission scanning electron microscopy (FE-SEM; HITACHI, S-4800). The crystal structures of asprepared samples were determined by an X-ray diffraction (XRD, BRUKER D8 ADVANCE) with Cu  $K_{\alpha}$  radiation. The elemental surface composition of the sample was analyzed by X-ray photoelectron spectroscopy (XPS) on a PHI 5700 ESCA System with an Al  $K_{\alpha}$  X-ray source. Light absorption properties were characterized by UV–vis diffuse reflection spectra (DRS) on a Hitachi U-4100 spectrophotometer.

#### 2.3. Photocatalytic hydrogen production experiments

Photocatalytic hydrogen production experiments were carried out in a quartz reactor. The prepared nanotube array films were immersed in  $36\,\mathrm{mL}$  H $_2\mathrm{O}$  and  $4\,\mathrm{mL}$  methanol anhydrous. The solution was irradiated by a  $350\,\mathrm{W}$  high-pressure Hg lamp, which was positioned  $10\,\mathrm{cm}$  away from the column reactor. Meanwhile, the reaction solution was stirred with a magnetic stirrer. The amount of generated hydrogen was measured by gas chromatograph (thermal conductivity detector, molecular sieve  $5\,\mathrm{\mathring{A}}$  column, Ar carrier).

#### 3. Results and discussion

#### 3.1. SEM images

Fig. 1(a) shows SEM image of  $Ta_2O_5$  nanotube arrays obtained by anodization. It can be seen that  $Ta_2O_5$  nanotubes could be formed by anodization of Ta foils. The lateral SEM image of  $Ta_2O_5$  nanotube arrays is shown in Fig. 1(b). The image shows that the diameter and length of the nanotubes were about 60 nm and 4  $\mu$ m, respectively. Moreover, a minor part of Ta substrate surface is visible. The inset shows the top view of an anodized Ta substrate surface. Based on the surface morphology of Ta substrate, the convex shape of the nanotube bottoms can be reflected. Moreover, the nanotubes are open on the top as shown in Fig. 1(c)–(e) shows the lateral and the top SEM images of  $Na_2Ta_2O_6$  nanotube arrays, respectively.

It can be seen that the nanotube structure can be clearly seen. The distribution and size of the pores are relatively uniform. The diameter and length of  $Na_2Ta_2O_6$  nanotube arrays are 50 nm and 4  $\mu$ m, respectively. The near-bottom morphology of  $Na_2Ta_2O_6$  nanotube arrays is shown in Fig. 1(f). Compared with Fig. 1(e), it is obvious that the porous diameters are smaller than the top diameters.

#### 3.2. X-ray diffraction

The XRD patterns of Ta<sub>2</sub>O<sub>5</sub> nanotube arrays and Na<sub>2</sub>Ta<sub>2</sub>O<sub>6</sub> nanotube arrays on Ta substrates are shown in Fig. 2. As can be seen from Fig. 2(a), no characteristic peaks of Ta<sub>2</sub>O<sub>5</sub> could be observed, showing that Ta<sub>2</sub>O<sub>5</sub> nanotube array film is amorphous. The presence of Ta diffraction peaks from the substrates is unavoidable due to the thin thickness of Ta<sub>2</sub>O<sub>5</sub> nanotube array film. For all the Na<sub>2</sub>Ta<sub>2</sub>O<sub>6</sub> samples, the main characteristic peaks can be indexed to a cubic structure of pyrochlore Na<sub>2</sub>Ta<sub>2</sub>O<sub>6</sub> (JCPDS Card No. 70-1155). It indicates that Ta<sub>2</sub>O<sub>5</sub> nanotube arrays can be thoroughly transformed to Na<sub>2</sub>Ta<sub>2</sub>O<sub>6</sub> nanotube arrays by the hydrothermal treatment. Compared with Fig. 2(b), it can be seen that the intensities of all characteristic peaks in Fig. 2(c) are stronger. It indicates that the crystallinity of the Na<sub>2</sub>Ta<sub>2</sub>O<sub>6</sub> nanotube arrays becomes higher with the increase of temperature. Moreover, with the increase of reaction time, the diffraction peaks become sharp and strong as shown in Fig. 2(d) and (e), suggesting that the Na<sub>2</sub>Ta<sub>2</sub>O<sub>6</sub> nanotube arrays can be crystallized well.

#### 3.3. X-ray photoelectron spectroscopy

In order to determine the chemical composition of the films and analyze the chemical state of the elements, XPS was carried out to analyze the Pt loaded Na<sub>2</sub>Ta<sub>2</sub>O<sub>6</sub> nanotube arrays. Fig. 3(a) shows that the sample is composed of Pt, Ta, Na, O and C. The peak observed at 285 eV corresponds to C 1s, resulting from carbon contamination of the film surface. Fig. 3(b) shows the typical XPS spectrum of Pt 4f core level. The spectrum can be well fitted with two Gaussian peaks. The doublet peaks appear at 71.1 and 75.1 eV, which can be attributed to the Pt  $4f_{7/2}$  and Pt  $4f_{5/2}$ levels of metallic Pt, respectively [29]. The binding energy indicates that metallic Pt is the predominant species with only a small contribution of oxidized state in the Pt loaded sample [30]. This suggests that the loaded Pt on the surface of Na<sub>2</sub>Ta<sub>2</sub>O<sub>6</sub> nanotube arrays is in the metallic form. The Ta 4f XPS spectrum fitted with two Gaussian peaks is shown in Fig. 3(c). Ta  $4f_{7/2}$  and Ta  $4f_{5/2}$  peaks appear at 26.1 and 28.0 eV, respectively, which indicates that the composition of the film is  $Ta^{5+}$  [31]. The narrow scan spectrum of O 1s is shown in Fig. 3(d). The O 1s XPS spectrum can be fitted with two components. The major peak of lower binding energy (530.8 eV) was assigned to the lattice oxygen (Ta-O bond) in Na<sub>2</sub>Ta<sub>2</sub>O<sub>6</sub>. The smaller peak located at 532.8 eV could be ascribed to the hydroxyl group or absorbed oxygen in the surface of the film [32].

#### 3.4. Optical-absorption properties

The UV–vis diffuse reflectance spectra of  $Na_2Ta_2O_6$  nanotube arrays and Pt loaded  $Na_2Ta_2O_6$  nanotube arrays are compared in Fig. 4(a). It can be seen that the spectrum of  $Na_2Ta_2O_6$  nanotube arrays is different from  $Pt-Na_2Ta_2O_6$  nanotube arrays. The optical absorption of  $Pt-Na_2Ta_2O_6$  nanotube arrays increases significantly in the region of 250-750 nm compared with  $Na_2Ta_2O_6$  nanotube arrays. This is attributed to the plasmon resonance of Pt particles deposited on  $Na_2Ta_2O_6$  nanotube arrays [33]. Surface plasmon resonance refers to the phenomenon in which the electromagnetic

#### Download English Version:

## https://daneshyari.com/en/article/1331381

Download Persian Version:

https://daneshyari.com/article/1331381

Daneshyari.com